ISSN 1063-7826, Semiconductors, 2021, Vol. 55, No. 3, pp. 319–327. © Pleiades Publishing, Ltd., 2021.
Russian Text © The Author(s), 2021, published in Fizika i Tekhnika Poluprovodnikov, 2021, Vol. 55, No. 3, pp. 241–250.

Features of Electron Transport in Two-Dimensional Quantum Superlattices with the Non-Associative Dispersion Law

M. L. Orlov[a,*] and L. K. Orlov[b,c]

[a] *Russian Presidential Academy of National Economy and Public Administration, Nizhny Novgorod, 603950 Russia*
[b] *Nizhny Novgorod State Technical University, Nizhny Novgorod, 603950 Russia*
[c] *Institute for Physics of Microstructures, Russian Academy of Sciences, Nizhny Novgorod, 603950 Russia*
**e-mail: orlov@ipm.sci-nnov.ru*

Received March 9, 2020; revised September 14, 2020; accepted October 26, 2020

Abstract—The anisotropy of the conductivity and the shape of the I–V characteristics for a two-dimensional quantum superlattice with the nonharmonic electron dispersion law are investigated for different directions of the current and field applied to the structure relative to the superlattice axes. The anisotropy of the characteristics and the conditions for the occurrence of multivalue I–V characteristics in different current flow modes are discussed. It is shown that the deviation of the electron dispersion law in a two-dimensional quantum superlattice from the harmonic one in a strong dc electric field noticeably affects the shape of the I–V characteristic of a two-dimensional quantum superlattice. Several current peaks in a strong field are caused by both mixing of the current lines for directions orthogonal to the applied field and electron transport over Stark-ladder levels formed in different miniband valleys.

Keywords: two-dimensional superlattices, non-associative dispersion law, anisotropy, dc electric field, I–V characteristic, Stark states

DOI: 10.1134/S1063782621030143

1. INTRODUCTION

Interest in two-dimensional (2D) heterocomposites and nanocomposites, in particular, quantum superlattices (SLs) is related, to a great extent, to the development of nanotechnology and advances in the development of nanotransistors, quantum cascade lasers, and quantum-dot lasers. The rapid development of the technology of bipolar and field-effect heterotransistors with the tunneling emission of electrons into the nanoscale base (channel) region of a structure makes the study of features in the characteristics of surface nanostructured periodic composites already relevant at the current stage. Now, it is most frequently suggested that 2D quantum SLs (2DSL) are formed using arrays of quantum dots and nanopores coupled by tunneling [1, 2]. In addition, it is interesting to study natural superstructures, which are implemented, e.g., on the basis of heterocomposites with nanocrystalline silicon-carbide layers [3]. At present, the possibilities of observing the spatial confinement effects in silicon-carbide nanocrystallites are widely discussed in publications [4]. The properties of various allotropic forms of silicon-carbide crystals characterized by the presence of a natural superlattice in the bulk of the structure have also been intensively investigated [3, 5]. Obviously, the development of such systems significantly expands the range of properties of available quantum electronic devices based on 1D superlattices and makes it possible to consider the characteristics of nanocrystalline materials from a new perspective.

The effect of Bloch generation, which has been experimentally studied in 1D GaAs/AlGaAs quantum superlattices since the 90s [6, 7], holds a special place among phenomena discussed in relation to periodic semiconductor heterostructures. Despite the difficulties faced in manufacturing a Bloch generator, it continues to attract the attention of numerous researchers due to the low level of critical fields of emission generation in it and the possibility of operation in the microwave range [8]. The interest related to 2D quantum SLs is due to the fact that, as was shown in [9], under certain conditions, they are characterized by long lifetimes of Bloch oscillations as compared with 1D periodic structures. This allows one to increase the lasing power and the efficiency of conversion of high-frequency radiation in 2DSLs, making them attractive for application.

Meanwhile, at present, the theoretical study of the electronic characteristics of 2D quantum SLs are limited to few works focused mainly on the simplest harmonic electron dispersion law in a SL in the form of a square [1, 2, 9, 10]. On the other hand, the effect of Bloch generation is related to electron transport in a narrow miniband and can depend on the electron dispersion law implemented in it in the applied electric-field direction. The diagnostics of the miniband spectrum and, correspondingly, identification of the lasing mechanism observed in the SL are, however, quite difficult, since in a strong electric field the electron dispersion law in a SL is transformed into a system of discrete levels, which generally form a system of Stark ladders [2, 11]. In view of this, studying the features of the response of a system to external perturbation caused by the effect of the initial (without electric field) form of the electron dispersion law on the Wannier–Stark quantization of the electron spectrum in the SL minibands is an important task.

In this study, we investigate the shape of the *I–V* characteristics of a 2DSL for different modes of current flow through the structure. The features of the anisotropy of the transport properties of lateral quantum SLs with a harmonic electron dispersion law more complex than a simple one in a dc electric field **E** are analyzed. The anisotropy of the conductivity and the mechanisms responsible for the manifestation of various features in the *I–V* characteristic are discussed. On the one hand, interest in SLs with a complex electron dispersion law is due to the wide range of semiconductor materials currently used in fabricating periodic heterostructures. On the other hand, the transport properties of carriers in 2DSLs in a strong dc electric field are greatly affected by the anisotropy of electron scattering, which causes mixing of the quantum states for different crystallographic directions. Therefore, additional mechanisms affecting the negative conductivity observed at both low and high frequencies can appear in the system.

2. ELECTRON TRANSPORT IN TWO-DIMENSIONAL SUPERLATTICES IN A STRONG DC ELECTRIC FIELD

Below, we examine features of the transport characteristics of lateral quantum 2DSLs in different current flow modes. In contrast to previous studies [1, 12, 13], which were devoted to a simple square lattice with a harmonic electron dispersion law, here we discuss the electrical characteristics of 2DSLs with a more complex quasimomentum dependence of the carrier energy. Let us write the electron dispersion law in a 2D miniband in the form

$$\begin{aligned}\varepsilon(\mathbf{k}) = \varepsilon(k_3) + \varepsilon(\mathbf{k}_\perp) = \varepsilon(k_3) + \Delta_1\{1 - [\Delta_{11}\cos(k_1 d_1) \\ + \Delta_{12}\cos(k_2 d_2)]/(\Delta_{11} + \Delta_{12})\} \\ + \Delta_2\{1 - \delta_0\cos(k_1 d_1)\cos(k_2 d_2)\},\end{aligned} \quad (1)$$

where $\varepsilon(\mathbf{k})$ and $\mathbf{k}$ are the electron energy and wave vector, respectively; k_i are its components; and $\Delta_{1(2)}$, Δ_{11}, Δ_{12}, and $\delta_0 = \pm 1$ are the parameters of the energy band of the 2D quantum SL. The introduction of the dissociative ($\sim\Delta_2$) term complicates the dispersion law, allowing the appearance of additional lateral extrema in the 2D Brillouin zone. The position of the latter is highly sensitive to the choice of both the parameters and the direction (the angle θ of the vector $\mathbf{k}$ relative to the principal axis x_1). In general, the $\varepsilon(\mathbf{k}_\perp)$ dependence is determined by the choice of materials for the heteropair. Representation of the $\varepsilon(k_3)$ dependence in the form $\varepsilon(k_3) = \hbar^2 k_3^2/2m_3^*$ can be used, for example, for 2DSLs consisting of a periodic set of 1D quantum wires arranged vertically and coupled by tunneling, which are formed in a nanoporous photonic crystal. Another example is textured polycrystals (for example, the 3*C*-SiC/Si(100) structures) with nanoscale grains growing in columns in the vertical growth direction [3]. In a 2D array of quantum dots, it is reasonable to assume $\varepsilon(k_3) = \varepsilon_{03} = \text{const}$, where ε_{03} corresponds to the lowest size-quantization level in the direction perpendicular to the 2DSL plane. In the general case, we assume $d_1 \neq d_2$, which is typical of quantum-dot arrays arranged along parallel guide grooves formed on the crystal surface, which are discussed in publications.

At the first stage, in order to identify the features caused by the specificity of the electron dispersion law, similar to [1, 12], we calculate the *I–V* characteristics of a 2D quantum SL using the Boltzmann equation with the collision integral in the constant relaxation-time approximation

$$\begin{aligned}\partial f/\partial t + (e/\hbar)E_1(t)\partial f/\partial k_1 + (e/\hbar)E_2(t)\partial f/\partial k_2 \\ = -(f - f^0)/\tau,\end{aligned} \quad (2)$$

where $f(k, t)$ and $f^0(k)$ are the nonequilibrium field-disturbed and equilibrium electron distribution functions, respectively. The approximation chosen for the collision integral is wholly acceptable for revealing the main features of the electrical characteristics related to the form of the electron dispersion law used in the lower miniband and simultaneously take into account the effect of the entanglement of states for different directions. Next, along with a 2DSL characterized by a square unit cell ($d_1 = d_2 = d$), which is natural, for example, for nanocrystalline textured 3*C*-SiC films deposited onto the Si(100) surface [3], we also consider the characteristics of SLs with a rectangular cell ($d_1 \neq d_2$). A version of the latter, as was mentioned above, are line structures consisting of a periodic sequence of quantum dots with the period d_1 formed along natural or artificial guides separated by dielectric layers.

In the one-miniband approximation, the equation for the current density is written in the form

$$\mathbf{j} = (e/4\pi^3\hbar)\int_\Omega f(\mathbf{k})(\partial\varepsilon/\partial\mathbf{k})\partial\mathbf{k}. \quad (3)$$

Using the periodicity condition, we present the distribution function as a Fourier series

$$f(k_1, k_2, t) = \sum_{\nu,\mu=-\infty}^{\infty} F_{\nu\mu}\Phi_{\nu\mu}(t)\exp\{i(\nu k_1 d_1 + \mu k_2 d_2)\}, \quad (4)$$

$$F_{\nu\mu} = (1/8\pi^3)\int_{-\infty}^{\infty}\partial k_3\int_0^{2\pi}\partial(k_1d_1)\int_0^{2\pi}\partial(k_2d_2)f^0(\mathbf{k}) \times \exp\{-i(\nu k_1d_1 + \mu k_2d_2)\}. \quad (5)$$

The expression for $F_{\nu\mu}$ depends on the dimensionality of the model and the choice of the equilibrium distribution function. For the Boltzmann distribution and dispersion law (1), we obtain

$$F_{\nu\mu} = F_0 \operatorname{Re}\int_0^{2\pi}\partial x_1\int_0^{2\pi}\partial x_2 \exp(i\nu x_1 + i\mu x_2) \times \exp\{Y_{11}\cos(x_1) + Y_{12}\cos(x_2) + Y_2\cos(x_1)\cos(x_2)\}, \quad (6)$$

where

$$x_{1,2} = k_{1(2)}d_{1(2)},$$
$$D_{10} = \Delta_1/\{(\Delta_{11} + \Delta_{12})\}, \quad D_{11} = D_{10}\Delta_{11},$$
$$D_{12} = D_{10}\Delta_{12}, \quad D_{20} = \delta_0\Delta_2, \quad Y_{ij} = D_{ij}/k_BT,$$
$$F_0 = \{(2\pi m_3k_BT)^{1/2}/16\pi^3\hbar\}\exp\{(\mu_F - \Delta_1 - \Delta_2)/k_BT\}.$$

When deriving Eq. (6), we assumed that the directions of vectors $\mathbf{k}_1$ and $\mathbf{k}_2$ coincide with the directions of the principal axes of the rectangular lattice: $\mathbf{k}_1 \parallel [100]$ and $\mathbf{k}_2 \parallel [010]$. The $\Phi_{\nu\mu}(t)$ function is determined by solving Eq. (2)

$$\Phi_{\nu\mu} = \exp\{-(t - t_0)/\tau\} + \tau^{-1}\int_{t_0}^{t}\exp\left\{(t' - t)/\tau - i(e/\hbar) \times \int_{t'}^{t}[\nu E_1(t'')d_1 + \mu E_2(t'')d_2]\partial t''\right\}\partial t'. \quad (7)$$

In the case of a dc electric field $\mathbf{E}$ = const with components $E_{1,2}$ along the $x_{1,2}$ axes, at the initial instant of the time of switching on the field $t_0 = -\infty$, we have

$$\Phi_{\nu\mu} = \{1 - i\tau[\nu\Omega_1 + \mu\Omega_2]\}/\{1 + \tau^2[\nu\Omega_1 + \mu\Omega_2]^2\}, \quad (8)$$

where $\Omega_1 = (ed_1/\hbar)E_1$, $E_1 = E\cos\psi$, $\Omega_2 = (ed_2/\hbar)E_2$, $E_2 = E\sin\psi$, $\Omega\tau = E/E_0$, $E_0 = \hbar/ed_1\tau$, and ψ is the angle between the field direction and axis x_1. Substituting (1), (4), (6), and (8) into Eq. (3), we arrive at expressions for the current components along the principal axes of the 2DSL with dispersion law (1). The corresponding equations for the current density components j_1 and j_2 in the direction of the 2DSL principal axes take the form

$$j_1 = j_0(E/E_0)\cos\psi\{D_{11}F_{10}/[1 + (E/E_0)^2\cos^2\psi] + F_{11}D_{20}\{1 + (E/E_0)^2 \times[\cos^2\psi - \chi\sin^2\psi]\}/\{1 + 2(E/E_0)^2 \times[\cos^2\psi + \chi\sin^2\psi] + (E/E_0)^4[\cos^2\psi - \chi\sin^2\psi]^2\}\}, \quad (9)$$

$$j_2 = j_0(E/E_0)\sin\psi\{D_{12}F_{01}/[1 + \chi(E/E_0)^2\sin^2\psi] + F_{11}D_{20}\{1 - (E/E_0)^2 \times[\cos^2\psi - \chi\sin^2\psi]\}/\{1 + 2(E/E_0)^2 \times[\cos^2\psi + \chi\sin^2\psi] + (E/E_0)^4[\cos^2\psi - \chi\sin^2\psi]^2\}, \quad (10)$$

where $j_0 = eF_0/2\pi\hbar d_2$ and $\chi = (d_2/d_1)^2$. If we introduce the parameter d_ψ corresponding to the SL period in the direction of the applied field $\mathbf{E}$ ($d_1 = d_\psi\cos\psi$, $E_\psi = \hbar/ed_\psi\tau$), then current components (9) and (10) can be rewritten as

$$j_1 = j_0(E/E_\psi)\{D_{11}F_{10}/[1 + (E/E_\psi)^2] + F_{11}D_{20}[1 + (E/E_\psi)^2 \times(1 - \chi\tan^2\psi)]/[1 + 2(E/E_\psi)^2(1 + \chi\tan^2\psi) + (E/E_\psi)^4(1 - \chi\tan^2\psi)^2]\}, \quad (11)$$

$$j_2 = j_0(E/E_\psi)\tan\psi\{D_{12}F_{01}/[1 + \chi(E/E_\phi)^2\tan^2\psi] + F_{11}D_{20}[1 - (E/E_\psi)^2(1 - \chi\tan^2\psi)]/[1 + 2(E/E_\psi)^2 \times(1 + \chi\tan^2\psi) + (E/E_\psi)^4(1 - \chi\tan^2\psi)^2]\}. \quad (12)$$

In formulas (9) and (11), the first terms in curly brackets describe the I–V characteristic of a 1D (along the x_1 axis) quantum SL. For a 2D quantum SL in the absence of a nonadditive term in dispersion law (1), i.e., at $D_{20} = 0$, current density equations (9) and (10) were obtained and investigated in [1]. In the work, the anisotropy of the electrical characteristics of a quantum SL was first studied. In particular, it was shown that the mixing of electronic states in the directions longitudinal and transverse relative to the field leads to a mismatch between the directions of the field and the current flowing through the structure. The degree of anisotropy increased with the applied electric field.

3. FEATURES OF THE I–V CHARACTERISTIC OF A TWO-DIMENSIONAL QUANTUM SUPERLATTICE WITH A NONADDITIVE DISPERSION LAW AT A SPECIFIED FIELD DIRECTION

Preliminary analysis of the I–V characteristic carried out in [12] for the simplest square lattice ($D_{11} = D_{12}$) showed that the presence of a nonadditive term ($\Delta_2 \neq 0$) in dispersion law (1) affects the I–V characteristic, shifting its maximum toward fields higher or lower than the nonlinearity critical field E_0. In strong fields, an additional (second) maximum may, in principle, appear in the I–V characteristic of a 2DSL with a nonadditive dispersion law. Below, we consider in more detail the properties of the steady-state conductivity and features of the I–V characteristic caused by the nonadditivity of the electron dispersion law in a 2DSL with both the same and different SL periods d_1 and d_2 along the principal symmetry axes.

In the general case, the value of the current flowing through the structure is expressed as $j = (j_1^2 + j_2^2)^{1/2}$

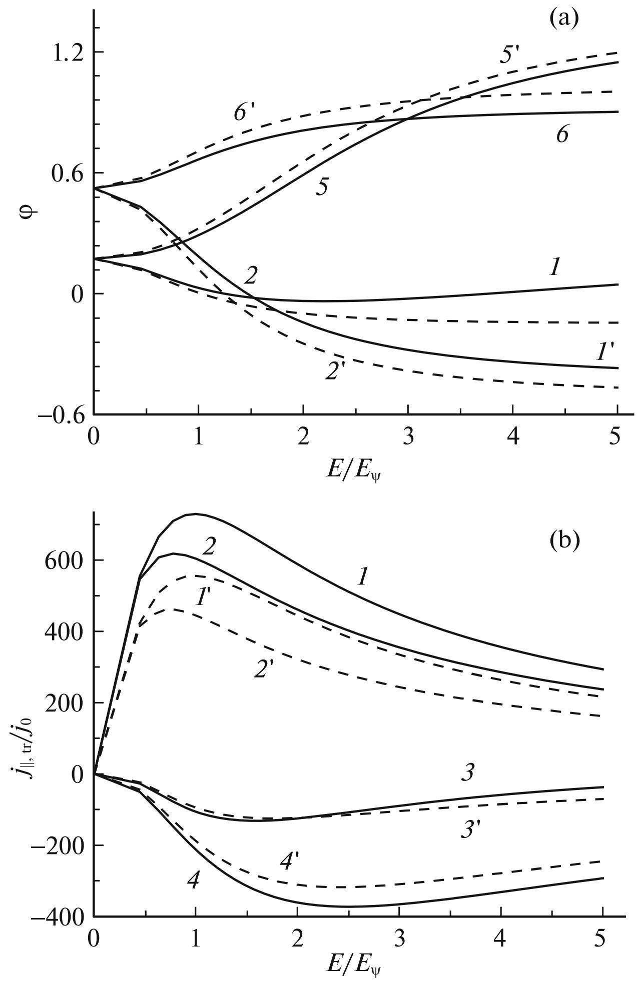

Fig. 1. Field dependences of the angle φ of inclination of (a) the current lines and (b) the values of the current components (*1*, *1'*, *2*, *2'*) parallel ($j_\parallel$) and (*3*, *3'*, *4*, *4'*) perpendicular (j_{tr}) to the field direction of the current components **j** for the angles ψ = (*1*, *1'*, *3*, *3'*, *5*, *5'*) $\pi/18$ and (*2*, *2'*, *4*, *4'*, *6*, *6'*) $\pi/6$. The parameters of a 2D square SL were taken to be $d_2 = d_1$, $\Delta_1 = 5$ meV, Δ_2 = (*5*, *5'*, *6*, *6'*) 1 and (*1–4*, *1'–4'*) 20 meV, $\Delta_{11}\Delta_{12} = 1$, δ_0 = (*1–6*, solid line) 1 and (*1'–6'*, dashed line) –1, and $k_BT = 7$ meV.

and the relation $j_2/j_1 = \tan\varphi$ sets the current direction relative to the x_1 axis, which is determined by the angle φ. As was already noted in [1, 12], the main feature of a 2DSL is the mismatch between the directions of the field (angle φ) and the current flowing through the structure (angle φ). For a 2D lattice, the exceptions are high symmetry axes, i.e., the angles $\psi = \varphi = 0, \pi/4$, and $\pi/2$ (at $d_1 = d_2$) and $\psi = \varphi = 0$ and $\pi/2$ (at $d_1 \neq d_2$). The mismatch between the angles ψ and φ is related to the asymmetry of the distribution function in the collision integral, which arises as a result of entanglement of the quasimomenta k_1 and k_2 upon heating of the electron gas. The asymmetry increases with applied electric field. In this case, the observed effect manifests itself even in structures with a purely harmonic dispersion law ($\Delta_2 = 0$) under the conditions of an isotropic relaxation time (τ = const) [1]. The observed divergence of the angles ψ and φ increases with deviation of the chosen field direction from the high symmetry axes and the value of the applied electric field.

3.1. Conductivity of Electrons in a Square Two-Dimensional Superlattice

For a square lattice with the parameters $\Delta_1 \gg \Delta_2$, the maximum current is obtained at angles (ψ, φ) lying in the diagonal direction ($\psi, \varphi \approx \pi/4$) at $\Omega\tau \approx \sqrt{2}$:

$$j \approx j_0(D_{11}F_{10} + D_{12}F_{01})(\Omega\tau/\sqrt{2})/[1 + (\Omega t)^2/2]. \quad (13)$$

For a lattice with the parameters $\Delta_1 \ll \Delta_2$, as well as for a 1D SL, the maximum current is obtained at angles (ψ, φ) close to zero at $\Omega\tau = 1$

$$j \approx j_0 F_{11} D_2 \Omega\tau/\{1 + (\Omega\tau)^2\}. \quad (14)$$

In the more general case, the characteristic dependences of the angle φ and the components of the current **j** flowing through the structure on the direction and value of the applied field **E** for a square SL are shown at several parameter values in Fig. 1. In a square SL, for all values of the parameters in the region of high fields $E > E_\psi$, the current steadily decreases with an increase in the electric field.

The presence of the nonadditive term ($\Delta_2 \neq 0$) in dispersion law (1) upon a deviation in the direction of the electric field applied to the structure from the principal symmetry axes ($\psi = 0, \pi/4$) leads to a change in the shape of the *I–V* characteristic, in particular, to the occurrence of a transverse current component. The latter can occur if there are effective mechanisms for the drainage of carriers at the ends of a system; i.e., there is strong surface recombination. Then, charges do not accumulate at the lateral surface and the applied field direction does not change. As follows from Fig. 1a, the angle φ will depend on both the value of the applied field (the difference between the angles ψ and φ increases with field) and the contribution determined by the value (Δ_2) and sign (δ_0) of the dissociative term in the electron dispersion law. In this case, with increasing field, the transverse current component behaves similarly to the longitudinal component, but with the maximum current shifted toward stronger fields. The presence of negative differential conductivity portions in both current components indicates the possibility of the amplification of high-frequency signals polarized in both the longitudinal and transverse directions relative to the direction of the applied dc electric field. A decrease in the contribution of the dissociative term to the dispersion law leads to a change in the sign of the transverse component of the current (Fig. 1a), which can be used to identify the electron dispersion law in a SL. The calculations made for a quantum SL with both narrow and

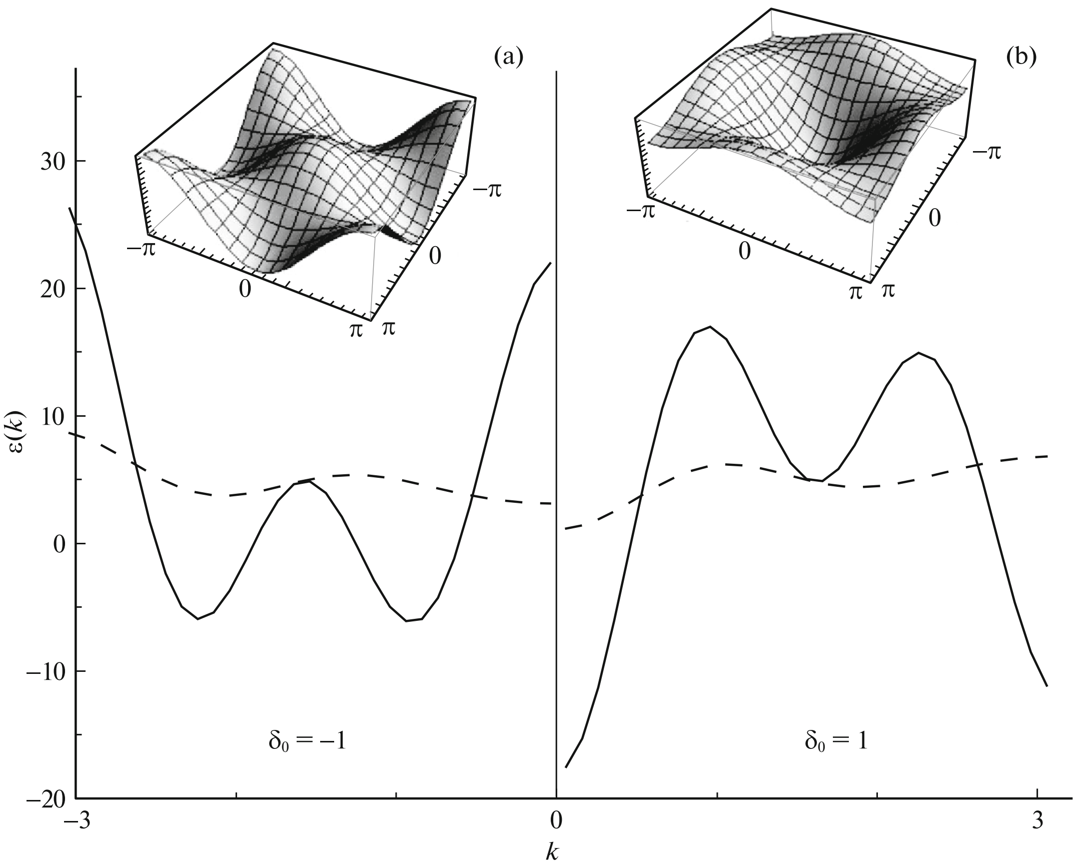

Fig. 2. General view of the dispersion law $\varepsilon(\mathbf{k})$ and its view in the direction at an angle of $\theta = \pi/10$ at parameters of $\Delta_1 = 5$ meV, $\Delta_{11} = \Delta_{12} = 1$, $\Delta_2 = 1$ (dashed line) and 20 meV (solid line), $\delta_0 =$ (a) −1 and (b) 1, and $k_BT = 7$ meV. Here, ε is given in meV and $k = k_{1,2}d_{1,2}$ is the dimensional parameter.

broad (relative to k_BT) allowed minibands in the region $\Omega\tau > 1$ show the dependence of the differential conductivity on the parameters included in the electron dispersion law. Thus, even within the quantum limit, the interrelation between the current flowing through the discrete levels of the Stark ladder and the form of the initial (without field) electron dispersion law in the miniband of the quantum SL is retained.

3.2. Conductivity of Electrons in a Two-Dimensional Superlattice with a Rectangular Lattice

A somewhat different situation is observed in a rectangular quantum SL ($d_1 \neq d_2$). In this case, the $\varepsilon(k)$ dependence contains lateral extrema, whose position and depth are determined by the value and sign of the parameter D_{20}, as well as by the choice of angle θ (Fig. 2). A change in the sign of the parameter δ_0 leads to inversion of the central valley, which can be of fundamental importance for periodic heterostructures with overlapping states of the valence and conduction bands of neighboring layers.

Figure 3 shows the field dependences of the current components in the longitudinal direction ($j_\parallel$) and the transverse direction (j_{tr}) relative to the applied electric-field direction at a fixed angle φ at different values of the dissociative term Δ_2 in the electron dispersion law. In the calculations, we took into account the effect of the amplitudes of the harmonics F_{IJ} included in the equations for the currents and changing with the parameters over a fairly wide range on the shape of the *I–V* characteristic. The comparison of the curves in Figs. 2 and 3 clearly demonstrates the interrelation between the dispersion law in the miniband, the chosen angle of application of the field, and the shape of the *I–V* characteristic of the SL.

It can be seen in Figs. 2 and 3 that the change in the form of the dispersion law with increasing parameter Δ_2 noticeably affects the transport properties of electrons in the SL. In this case, the inversion of the central valley upon a simple change in the sign of parameter δ_0 does not fundamentally affect the qualitative form of the *I–V* characteristic of the SL. The negative differential conductivity (NDC) portion observed in the *I–V* characteristic $j_\parallel(E)$ at $\Omega\tau \gg 1$ (Fig. 2) related to

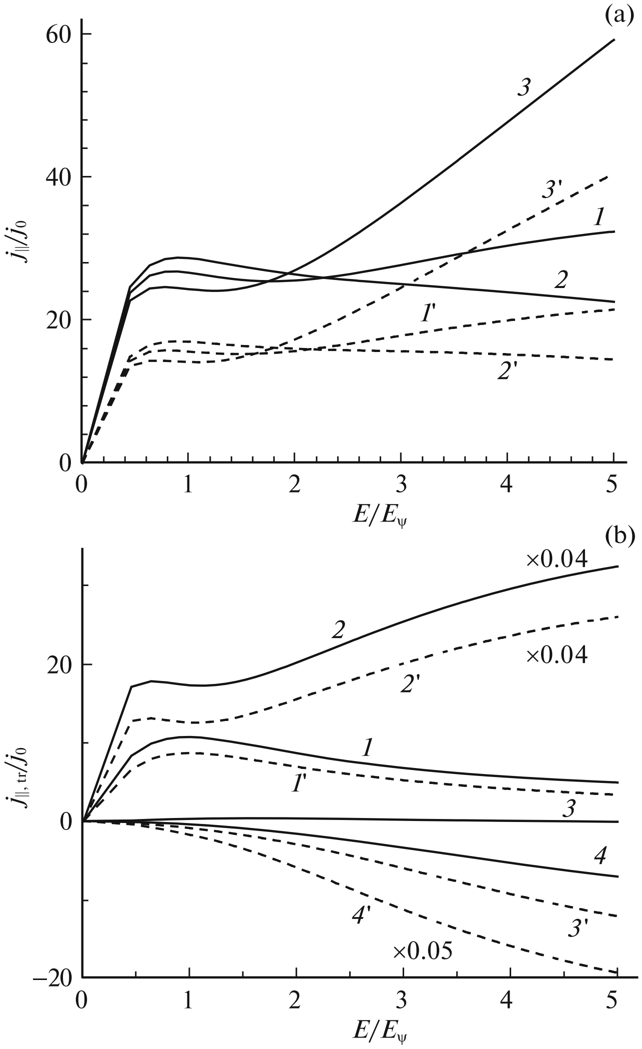

Fig. 3. Field dependences of the current components for several values of parameter Δ_2 and several constant angles ψ of field inclination. (a) Component $j_\parallel$, $\psi = $ (*1*, *1'*) $\pi/10$, (*2*, *2'*) $\pi/11$, and (*3*, *3'*) $\pi/9$; $\Delta_2 = 5$ meV; $\delta_0 = $ (*1–3*, solid curve) and (*1'–3'*) -1. (b) (*1*, *1'*, *2*, *2'*) component $j_\parallel$ parallel to the field direction and ((*3*, *3'*, *4*, *4'*) perpendicular component j_{tr}; $\psi = \pi/10$, $\Delta_2 = $ (*1*, *1'*, *3*, *3'*) 1 and (*2*, *2'*, *4*, *4'*) 20 meV; and $\delta_0 = $ (*1–4*, solid line) 1 and (*1'–4'*, dashed line) -1. The remaining parameters were taken to be $d_2/d_1 = 2.7$, $\Delta_1 = 5$ meV, $\Delta_{11} = \Delta_{12} = 1$, and $k_BT = 7$ meV.

the mechanism of Bloch oscillations noticeably narrows both with an increase in the dissociative term proportional to Δ_2 and upon a variation in the angle φ (Fig. 2a). In a strong field ($E > E_\psi$, with increasing parameter Δ_2, the current density increases, leading to the occurrence of an additional broad maximum in the current characteristic, which most likely results from the redistribution of electrons between neighboring valleys. In a strong field, the *I–V* characteristic of the 2DSL becomes similar to the characteristic of a 1D SL, which reveals the effective redistribution of electrons between adjacent minibands due to tunneling between them [11, 14, 15]. We can assume that, in a 2DSL with a complex multivalley dispersion law, the electron spectrum in a strong field transforms not into one, but into a system of Stark ladders, the transitions between which lead to the observed change in the shape of the *I–V* characteristic. To reduce the contribution of electrons in the lateral valleys to the formation of the *I–V* characteristic of a 2DSL, it is sufficient to change the angle of the applied field relative to the principal axes of the 2DSL (Fig. 2a). The possible entanglement caused by the anisotropy of the collision integral of states in the directions perpendicular to the field can also be assumed as the mechanism responsible for the appearance of the second maximum in the 2DSL *I–V* characteristic. This effect leads to mixing of the longitudinal and transverse conductivity of the system, similar to how it occurs in measurements of the quantum Hall effect by the van der Pauw method on a square probe [16]. The effect of the damping of Bloch oscillations due to the entanglement of Stark states in directions along and across the direction of current flowing in the structure was first discussed in [2, 9]. Obviously, more detailed information on the structure of quantum states in a SL in a dc electric field can only be obtained by analyzing simultaneously the high-frequency resonance characteristics of the system, as was done, for example, for a 1D quantum SL [17].

4. FEATURES OF THE *I–V* CHARACTERISTIC OF A TWO-DIMENSIONAL QUANTUM SUPERLATTICE IN THE FIXED CURRENT DIRECTION MODE

Above, we examined the situation corresponding to the choice of a specified field direction relative to the 2DSL axes. This mode can be implemented using a surface slot diode configuration by placing, for example, a planar SL between the source and drain contacts of a field-effect transistor. In a real experiment, however, the case of the absence of an effective recombination sink at the lateral ends of the structure can also be implemented. Then, due to charge accumulation at the lateral faces, the field will deviate from its initial direction and an electric-field component transverse to the current direction will arise [1]. In view of this, it seems necessary to consider the situation of a fixed current direction ($\varphi = \mathrm{const}$). Further, we assume that the current direction is specified and the angle φ is equal to the angle between the vectors $\mathbf{j}$ and $\mathbf{x}_1$. This mode is implemented, for example, on samples made in the Hall-bridge configuration. In this case, the field direction in the sample determined by the angle φ will depend on both the field value and other parameters of the system.

To calculate the *I–V* characteristic of a 2DSL for a fixed current direction, we can use Eqs. (11) and (12), which establish the dependence of the current component $j_\parallel$ on angle ψ at a specified applied electric-field value. Then, using the relation between the angles φ and ψ (see the inset in Fig. 4) determined at a constant field value by the relation $\varphi = \arctan(j_2/j_1)$, it is easy to establish the dependence of the total current j on the angle φ. Then, according to the obtained dependences, we select the current j and the longitudinal (along the current direction) field component $E_\parallel$ at fixed values of the field E and the angle φ (points in Fig. 4).

To carry out a more accurate analysis, let us consider the solutions of current transport equations (11) and (12), fixing the current direction, i.e., setting φ = const. Then, according to the preliminary analysis carried out in [4, 8], similar to the Hall effect, a field component directed across the current flowing through the sample will arise in the system. Let the direction of the current flowing through the structure be deviated from one of the SL principal axes (the x_1 axis) by angle φ which lies in the angular range between 0 and π/4. In this case, the longitudinal (**E**$_\parallel$ ∥ **j**) and transverse (**E**$_\perp$ ⊥ **j**) components of the electric field **E** and current **j** are related to their projections onto the SL principal axes by the relations

$$j_1 = j\cos\varphi, \quad j_2 = j\sin\varphi,$$
$$E_\parallel = E\cos(\psi - \varphi), \quad E_\perp = E\sin(\psi - \varphi). \tag{15}$$

The interrelation between the direction (angle ψ) and the field value E at a specified angle φ can be established using the condition of the zero tangential component of the current: $\tan\varphi = j_2/j_1 = \text{const}$. The desired $j_\parallel(E_\parallel)$ dependence is found by substituting the determined relation between E and ψ into the expression for the current density $j = j_\parallel = (j_1^2 + j_2^2)^{1/2}$, where $j_{1,2}$ are determined by Eqs. (11) and (12).

Let us consider first the simplest case φ = 0. In this case, using the condition $j_2 = 0$, we immediately find one solution $\psi^{(1)} = 0$, which corresponds to current and field coinciding in direction. Then, the expression for the current density takes the form

$$j^{(1)} = j_1 = j_{01}\Omega^{(1)}(D_{11}F_{10} + F_{11}D_{20})/\{1 + (\tau\Omega^{(1)})^2\}. \tag{16}$$

However, the condition of the zero current component j_2 allows also the existence of another solution. The simplest solution takes place at the transition to a SL with a predominantly dissociative dispersion law. In particular, at $\Delta_{12} = 0$, the relation between the $\psi^{(2)}$ direction and the field value $E^{(2)}$ has the form $\psi^{(2)} = \pm 1/2\arccos[1/(\tau\Omega^{(2)})^2]$; consequently, we have

$$j^{(2)} = j_{01}\Omega_\parallel^{(2)}(D_{11}F_{10} + F_{11}D_{20})/2;$$
$$\Omega_\parallel^{(2)} = \Omega^{(2)}\cos\{0.5\arccos[1/(\tau\Omega^{(2)})^2]\}. \tag{17}$$

The relation between the angle ψ (at 0 < ψ < π/2) and the Bloch frequency Ω, as well as the dependences of the current (at φ = 0) on the field component $E_\parallel$

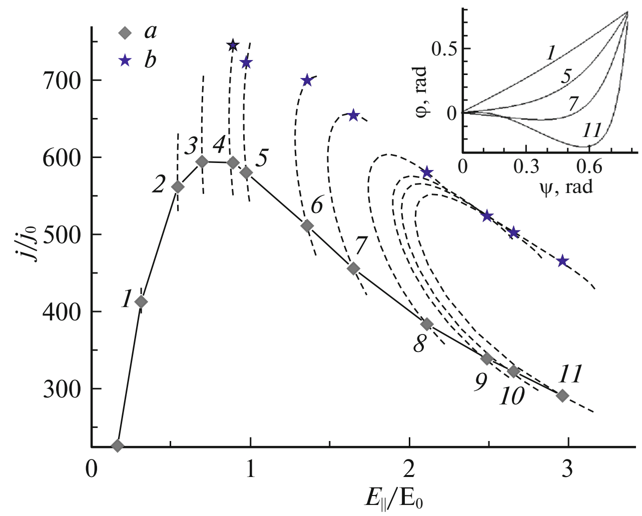

Fig. 4. Dependences of current j in the structure on the field component $E_\parallel$ parallel to the current at a constant angle of φ = 0.4 rad for a square SL with parameters of $d_2/d_1 = 1$, $\Delta_1 = 5$ meV, $\Delta_{11} = \Delta_{12} = 1$, $\Delta_2 = 20$ meV, and $\delta_0 = 1$ at $k_BT = 7$ meV in applied fields of $(E/E_0)^2 = $ (*1*) 0.1, (*2*) 0.3, (*3*) 0.5, (*4*) 0.8, (*5*) 1, (*6*) 2, (*7*) 3, (*8*) 5, (*9*) 7, (*10*) 8, and (*11*) 10. Inset: dependences of the angle φ of inclination of the current lines on angle ψ of inclination of the current lines for several $(E/E)^2$ values. Dashed curves show the $j(E)$ dependences for a constant field direction. Points correspond to the current values at (a) a constant field value and (b) a constant ψ value.

parallel to the current, which are described by Eqs. (16) and (17), are shown in Fig. 5a (curves *1*).

At $\Delta_{12} \neq 0$ and φ = 0 in the SL with a square Brillouin zone, the equation relating the direction of the field (angle ψ) with its value E/E_0 has the form of a quadratic equation with respect to both the variable $\Phi = \cos 2\psi$ and the variable $W = (E/E_0)^2$

$$D_{12}F_{01}[1 + 2W + W^2\cos^2 2\psi] + F_{11}D_{20}(1 - W\cos 2\psi)[1 + W/2 - (W/2)\cos 2\psi] = 0. \tag{18}$$

Solving Eq. (18), we find $\psi = \pm 0.5\arccos(\Phi)$, where $\Phi = \{-b \pm [b^2 - 4ac]^{1/2}\}/2a$, $a = W^2(D_{12}F_{01} + D_{20}F_{11}/2)$, $b = -F_{11}D_{20}(3 + W)W/2$, and $c = D_{12}F_{01}(1 + 2W) + F_{11}D_{20}(1 + W/2)$. Substituting the obtained solution into Eq. (11), we can easily calculate the field dependences of the current $j_1(E_1)$ and the transverse field component $E_2(E_1)$ (curves *2* in Fig. 5a).

At $\Delta_{12} \neq 0$ and φ = 0 in a SL with a rectangular lattice ($d_2/d_1 \neq 1$), the equation relating the field direction (angle ψ) and the field value $E_\parallel/E_\psi$ also has the form of a quadratic equation for the quantities $Z = \chi\tan^2\psi$ and $W = (E/E_\psi)^2$

$$A_1[1 + 2W(1 + Z) + W^2(1 - Z)^2] + A_2[1 - W + WZ][1 + WZ] = 0, \tag{19}$$

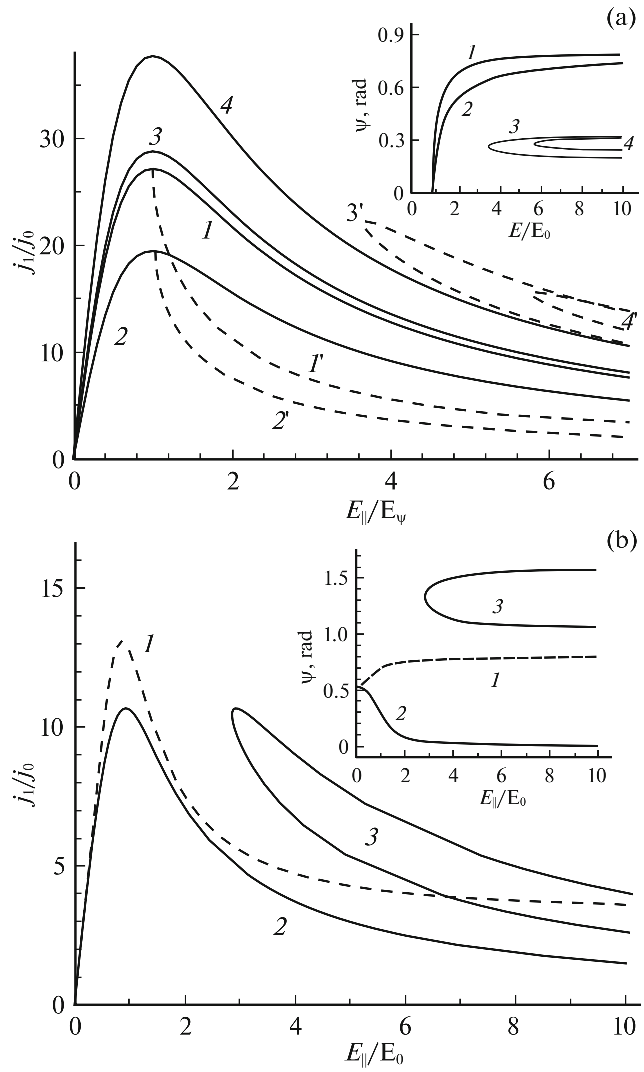

Fig. 5. Dependences of the current $j = j_1$ in the structure on the longitudinal field component $E_\|$ at constant angles of φ = (a) 0 and (b) $\pi/6$ and parameters of $\delta_0 = 1$, $\Delta_{11} = 1$, $k_BT = 7$ meV. (a) Δ_1 = (*1*, *3*, *4*) 5 and (*2*) 1 meV; Δ_{12} = (*1*, *1'*) 0, (*2*, *2'*, *3*, *3'*) 1, (*4*, *4'*) 3, and (*4*, *4'*) 3; Δ_2 = (*1*) 20, (*2*) 7, and (*3*, *4*) 5 meV. (b) $\Delta_{12} = 1$; (*1*) $\Delta_1 = 0$ and Δ_2 = 5 meV, (*2*, *3*) $\Delta_1 = 5$ meV and $\Delta_2 = 0$; (*2*) the main and (*3*) additional solutions. (a) (*1*, *2*) Square SL ($d_2/d_1 = 1$) and (*3*, *4*) rectangular SL ($d_2/d_1 = 3/1$). (b) Square SL ($d_2/d_1 = 1$). Insets: corresponding dependences of the angle ψ of inclination of the current lines on applied field E.

where $\chi = (d_2/d_1)^2$, $A_1 = \Delta_{12}F_{01}$, and $A_2 = \Delta_2F_{11}$. Solving Eq. (19), we find $\psi = \pm\arctan(Z/\chi)$, where $Z = \{-b \pm [b^2 - 4ac]^{1/2}\}/2a$, $a = W^2\{A_1 + A_2\}$, $b = -W^2(2A_1 + A_2) + 2W(A_1 + A_2)$, and $c = A_1(1 + W)^2 + A_2(1 - W)$, and substituting the obtained solution into Eq. (11), we can easily find the $j_1(E_1)$ and $E_2(E_1)$ dependences (curves *3* and *4* in Fig. 5a).

For an arbitrary angle φ, the problem is complicated, since it requires the solution of a third-order equation that relates the parameters W and ψ. In the general case, you can use also the procedure considered above when constructing the curves shown in Fig. 4. The obtained equation is solved most simply only in two special cases corresponding to the zero values of one of the parameters Δ_2 or Δ_1. These conditions correspond to the purely associative or purely dissociative electron dispersion law. In these cases, the relation between the value and direction of the applied field at $d_1 = d_2 = d$ takes the form

$$\tau^2\Omega^2 = \{D_{11}F_{10}\cos\psi - \sin\psi D_{12}F_{01}\}/\{D_{12}F_{01}\cos\psi - D_{11}F_{10}\sin\psi\}\sin\psi\cos\psi, \quad (20)$$

at $\Delta_2 = 0$ and

$$\tau^2\Omega^2 = (\tan\psi - \tan\varphi)/(\tan\psi + \tan\varphi)\cos 2\psi, \quad (21)$$

at $\Delta_1 = 0$. A typical form of the dependences of the angle ψ of inclination of the field lines and the value of the flowing current $j = j_\|$ on the value of the field $E_\|$ along the current lines at a specified angle $\varphi = \pi/6$ and the parameters $\Delta_{11} = \Delta_{12} = 1$, $\delta_0 = 1$, $k_BT = 7$, ($\Delta_1 = 0$, $\Delta_2 = 5$ meV) (dashed line *1*), ($\Delta_1 = 5$ meV, $\Delta_2 = 0$) (solid lines *2* (main solution) and *3* (additional solution) are shown in Fig. 5b. The change in the sign of the parameter δ_0 affects insignificantly the form of the curves shown in Fig. 5.

The decomposition of the current characteristic into several branches, which was first noted in [1], is accompanied by the occurrence of an electric-field component transverse in relation to the current direction, which can affect the behavior of the high-frequency characteristics. Despite the existence of several branches of the current characteristic, the system, however, will remain stable due to the presence of a balance bar, which is the transverse electric field. The deviation of the current leads to instantaneous occurrence of the field component $E_\perp$, which counteracts the occurrence of the transverse current component and the recovery of equilibrium in the system, which corresponds to the requirement for the constant direction of current flowing through the structure (in the investigated case, to the condition $\varphi = 0$). As a result, the jumps between different branches of the current will be short-term and the field direction will oscillate on both sides of the specified direction of the current with angles $\pm\psi$.

5. CONCLUSIONS

The features of the anisotropy and transport properties of lateral 2D quantum SLs with a complex multivalley dispersion law of electrons in the 2DSL lower miniband were analyzed. The anisotropy of the spectrum of a quantum SL in a strong dc electric field through the collision integral leads to the mixing of quantum levels of Stark ladders in the directions along and across the current flow lines. Mixing of the Stark levels noticeably affects the shape of the I–V characteristic, leading, in the case of a square SL, to slowing of the current drop in fields above the critical one ($E > E_0$). In a rectangular SL, in some cases, the current growth and the occurrence of an additional broad maximum in the I–V characteristic of a SL in strong fields at certain current flow angles can be observed. This effect is similar to the effect of tunneling breakdown between the levels of Stark ladders of adjacent minibands, which is observed in the I–V characteristics of 1D SLs. It can be assumed that, in 2DSLs, this feature of the I–V characteristic of a SL is related to electron transport between the levels of a series of Stark ladders forming in the Brillouin zone from groups of carriers localized in neighboring valleys. It was shown that the initial form of the electron dispersion law in the miniband noticeably affects the formation of Stark levels and the character of Bloch oscillations, which is reflected in the behavior of the response of the system to an external field.

ACKNOWLEDGMENTS

This study is devoted to the memory of Prof. Yu.A. Romanov, who initiated the formulation of the problem and the beginning of its solution.

FUNDING

This study was supported by the Russian Foundation for Basic Research, project no. 18-42-520062.

CONFLICT OF INTEREST

The authors declare that they have no conflict of interest.

REFERENCES

1. Yu. A. Romanov and E. V. Demidov, Semiconductors **31**, 252 (1997).
2. I. A. Dmitriev and R. A. Suris, Semiconductors **35**, 212 (2001).
3. L. K. Orlov, V. I. Vdovin, N. L. Ivina, Phys. Solid State **61**, 1263 (2019).
4. J. Y. Fan, X. L. Wu, and P. K. Chu, Progr. Mater. Sci. **51**, 983 (2006).
5. V. I. Sankin and A. A. Lepneva, Semiconductors **34**, 803 (2000).
6. C. Waschke, H. G. Roskos, R. Schwedler, K. Leo, H. Kurz, and K. Koler, Phys. Rev. Lett. **70**, 3319 (1993).
7. E. Schomburg, R. Scheuerer, S. Brandl, K. F. Renk, D. Pavel'ev, Yu. Kochurinov, V. Ustinov, A. Zhukov, A. Kovsh, and P. S. Kop'ev, Electron. Lett. **35**, 1491 (1999).
8. Yu. A. Romanov, L. G. Mourokh, and N. J. M. Horing, J. Appl. Phys. **93**, 4696 (2003).
9. I. A. Dmitriev and R. A. Suris, Semiconductors **36**, 1364 (2002).
10. S. Yu. Glazov and S. V. Kryuchkov, Semiconductors **35**, 444 (2001).
11. L. K. Orlov, Izv. Vyssh. Uchebn. Zaved. SSSR, Radiofiz. **32**, 1550 (1989).
12. M. L. Orlov, Yu. A. Romanov, and L. K. Orlov, Microelectron. J. **36**, 396 (2005).
13. M. L. Orlov, Yu. A. Romanov, and L. K. Orlov, in *Proceedings of the 1st International Workshop on Semiconductor Nanocrystals* (Budapest, Hungary, 2005), Vol. 2, p. 325.
14. L. K. Orlov and Yu. A. Romanov, Sov. Phys. Semicond. **19**, 1157 (1985).
15. L. K. Orlov, Radiotekh. Elektron. **33**, 1278 (1988).
16. O. A. Mironov, O. A. Kuznetsov, L. K. Orlov, R. A. Rubtsova, A. L. Chernov, S. V. Chistyakov, M. Oszwaldovskii, B. A. Aronzon, and N. K. Chumakov, Superlatt. Microstruct. **10**, 467 (1991).
17. L. K. Orlov and Yu. A. Romanov, Izv. Vyssh. Uchebn. Zaved. SSSR, Radiofiz. **32**, 282 (1989).

Translated by E. Bondareva